ELSEVIER

Journal of Materials Processing Technology 161 (2005) 415–422

Journal of Materials Processing Technology

www.elsevier.com/locate/jmatprotec

Understanding AlN sintering through computational thermodynamics combined with experimental investigation

M. Medraj[a,*], Y. Baik[b], W.T. Thompson[c], R.A.L. Drew[d]

[a] *Concordia University, Montreal, Canada QC, H3G 1M8*
[b] *Samsung Electronics Co., Gumi, Korea*
[c] *Royal Military College, Kingston, Canada*
[d] *McGill University, Montreal, Canada*

Received 23 July 2003; received in revised form 23 July 2003; accepted 27 May 2004

Abstract

Aluminum nitride (AlN) has attracted large interest recently as a suitable material for hybrid integrated circuit substrates because of its high thermal conductivity, high flexural strength, good dielectric properties, thermal expansion coefficient matches that of Si and non-toxic nature. Yttria (Y_2O_3) is the best additive for AlN sintering. Binary diagrams of Al_2O_3–Y_2O_3, AlN–Al_2O_3, and AlN–Y_2O_3 were thermodynamically modelled. The obtained Gibbs free energies of components, stoichiometric phases and solution parameters were used to build a thermodynamic database of AlN–Al_2O_3–Y_2O_3 system.

Liquid-phase sintering of AlN with Y_2O_3 as an additive has been studied and compared with the thermodynamic results. Sintering was performed in the temperature range of 1750–1950 °C for upto 4 h under a N_2 atmosphere to optimise the sintering conditions for each composition. The relative density exceeded 95% for all the compositions sintered at 1850 °C and full densification was achieved for all four compositions sintered at 1900 °C. The microstructure and assemblage of the secondary phase have a significant effect on the final thermal conductivity of the sintered AlN. Thermodynamic modelling of AlN–Al_2O_3–Y_2O_3 system provided an important basis for understanding the sintering behaviour and interpreting the experimental results.

Keywords: AlN sintering; Thermodynamic modeling; AlN–Al_2O_3–Y_2O_3 phase diagram

1. Introduction

Aluminum nitride (AlN) is currently used in electronic packaging and as an engineering ceramics. The thermal conductivity of an AlN single crystal (320 W/m K) is sixteen times higher than that of Al_2O_3 at room temperature and almost equal to that of 99.5% pure BeO at 150 °C. The coeffecient of thermal expansion, CTE, of AlN (4.4×10^{-6}/°C) is not only lower than both Al_2O_3 and BeO, but also closer to that of Si (3.2×10^{-6}/°C). Comparing the requirements for substrate materials with the properties of Al_2O_3 and BeO, shows that AlN can replace the widely used Al_2O_3 because of its thermal conductivity and its CTE and BeO because of its CTE and its non-toxic nature [1–4].

Since AlN is a covalently bonded material, it has a low diffusivity and requires high temperatures (1600–2000 °C) for sintering [5]. Moreover, in the presence of oxide on the powder surface and dissolved oxygen in the lattice, it is impossible to achieve a high thermal conductivity without the use of sintering additives. However, high density can be achieved in the absence of an additive due to the effect of surface Al_2O_3 that promotes densification. To enhance the thermal conductivity of AlN, it is necessary to use additives. The sintering of AlN with an additive is usually performed at 1450–2000 °C for 1–6 h under N_2 atmosphere. Yttria (Y_2O_3) is the best additive for AlN sintering, and it has been shown that AlN densifies by a liquid phase mechanism, where the surface oxide, Al_2O_3, reacts with the oxide additive, Y_2O_3, to form a Y–Al–O–N liquid that promotes particle rearrangement and densification [6]. Experimental and thermodynamic explanation for the effect of the amount of Y_2O_3 additive on the secondary

* Corresponding author. Tel.: +1 514 848 2424x3146.
E-mail address: mmedraj@me.concordia.ca (M. Medraj).

0924-0136/$ – see front matter © 2004 Elsevier B.V. All rights reserved.
doi:10.1016/j.jmatprotec.2004.05.031

phase formation, densification and thermal conductivity will be presented in this work.

To date, there is little information on the ternary AlN–Al_2O_3-sintering additives system [7] and in spite of the large interest attracted over the last years by the excellent properties of AlN sintered by Y_2O_3, no attempts have been made up to now to construct the AlN–Al_2O_3–Y_2O_3 ternary phase diagram. To calculate reliable ternary, quaternary, and higher order metallic and ceramic phase diagrams, we need thermodynamic description of the binary phase diagrams and a thermodynamic model that can extrapolate binary data reliably into ternary and higher-order systems [8]. This is commonly done for metals where the thermodynamic data are more readily available. For ceramic systems, thermodynamic data are very sparse. Furthermore measurements are very difficult considering the high temperatures involved.

2. Thermodynamic modeling of AlN–Al_2O_3–Y_2O_3 system

There is an increasing demand for the development of thermodynamic databases, which are practically useful. A simple model is preferable to one, which is unnecessarily complex and is based on speculation about ionic structure of the phases. A database for AlN–Al_2O_3–Y_2O_3 system was built using FACT system [9]. Details of the thermodynamic modelling and the experimental investigation of the system using in situ neutron diffraction were published earlier [10,11].

The storage, retrieval and manipulation of thermodynamic data with the aid of the computer require accurate analytical representation of thermodynamic properties of solutions. Values of the standard Gibbs energies, G°, of each component are entered and stored in the solution database along with parameters which define the Gibbs energy of mixing according to Kohler/Toop polynomial model. In the present treatment the ternary excess Gibbs energy was calculated solely from a binary data interpolation. Binary terms of the polynomial expansion for G^E were entered as Redlich–Kister or Legendre polynomials due to their simplicity and the fact that their functional form is consistent with the empirical observations of solutions behaviour [12].

The ternary phase diagrams were calculated by taking all the thermodynamic data stated for the binary phases into consideration. The calculated isothermal sections of AlN–Al_2O_3–Y_2O_3 system are given in Fig. 1.

Fig. 1(a) shows the isothermal section at 2000 °C, which is below the temperature at which the primary crystallization of the three components occurs. This isothermal section shows that beside the region of the melt, the heterogeneous regions of the primary crystallization of AlN, Al_2O_3, Y_2O_3 and AlN polytypes exist in equilibrium with the liquid phase. In addition, two small three-phase areas of L + 27R + AlN and L + 21R + 27R are found. At 1900 °C, Fig. 1(b) most of the binary eutectic points of the system have appeared. There are seven areas of binary eutectic crystallization (i.e. L + two crystalline phases). Also a new primary solidification for YAM, YAP and YAG occurred at this temperature. At 1800 °C, the isothermal section can be seen in Fig. 1(c). It can be seen that the region of the melt shrinks, however at this temperature the liquid is still in equilibrium with the other phases in two and in three phases regions. At this temperature, the eutectic point between Al_2O_3 and YAG is encountered as it can be seen from the region of L + YAG + Al_2O_3. Also, there are still regions of primary solidification of AlN, YAG, Spinel, and Al_2O_3 in equilibrium with the melt. A later stage of solidification (1700 °C) is shown in Fig. 1(d), where there is no residual liquid. At this temperature, there are five three-crystalline-phases regions and one two-crystalline-phases region.

Table 1
Amount of Y_2O_3 additive in each sample

Composition	Y_2O_3 content (wt.%)
I	1.36
II	3.04
III	3.47
IV	7.59

3. Experimental procedure

AlN powder, Grade F (Tokuyama Soda, Japan) containing <0.9 wt.% of oxygen, <400 ppm of carbon, and trace amounts of other impurities (<60 ppm of Ca, <10 ppm of Fe, <15 ppm of Si), was used. The powder had a mean particle size of <0.3 μm and a specific surface area of 3.3 m^2/g. The Y_2O_3 powder (Grade 5630X, Union Molycorp, USA) had a mean agglomerate size of 1.8 μm and specific surface area of 33 m^2/g.

The amount of Y_2O_3 required as a sintering additive depends on the quantity of oxygen present in the AlN powder. The amount of Al_2O_3 in each sample was calculated according to the following chemical equation:

$$\frac{3}{2}O_2 + 2Al \rightarrow Al_2O_3 \quad (1)$$

assuming that all the oxygen in AlN powder is present in the form of Al_2O_3. The total oxygen level in the AlN powder was analysed after milling and drying by ELKEM Metals in Niagara Falls (New York) using a TC136 LECO EF100 electrode furnace and associated analyser. The AlN powder was mixed with various amounts of Y_2O_3 powder as shown in Table 1. The pre-mixed compositions were ball milled in a plastic container for 24 h using 3 mm diameter ZrO_2 media and reagent grade isopropanol with a solid to liquid ratio of 1:5 by volume. After milling for 24 h, the mixtures of AlN and Y_2O_3 were dried in a microwave oven to completely remove the isopropanol. The mixtures were then granulated

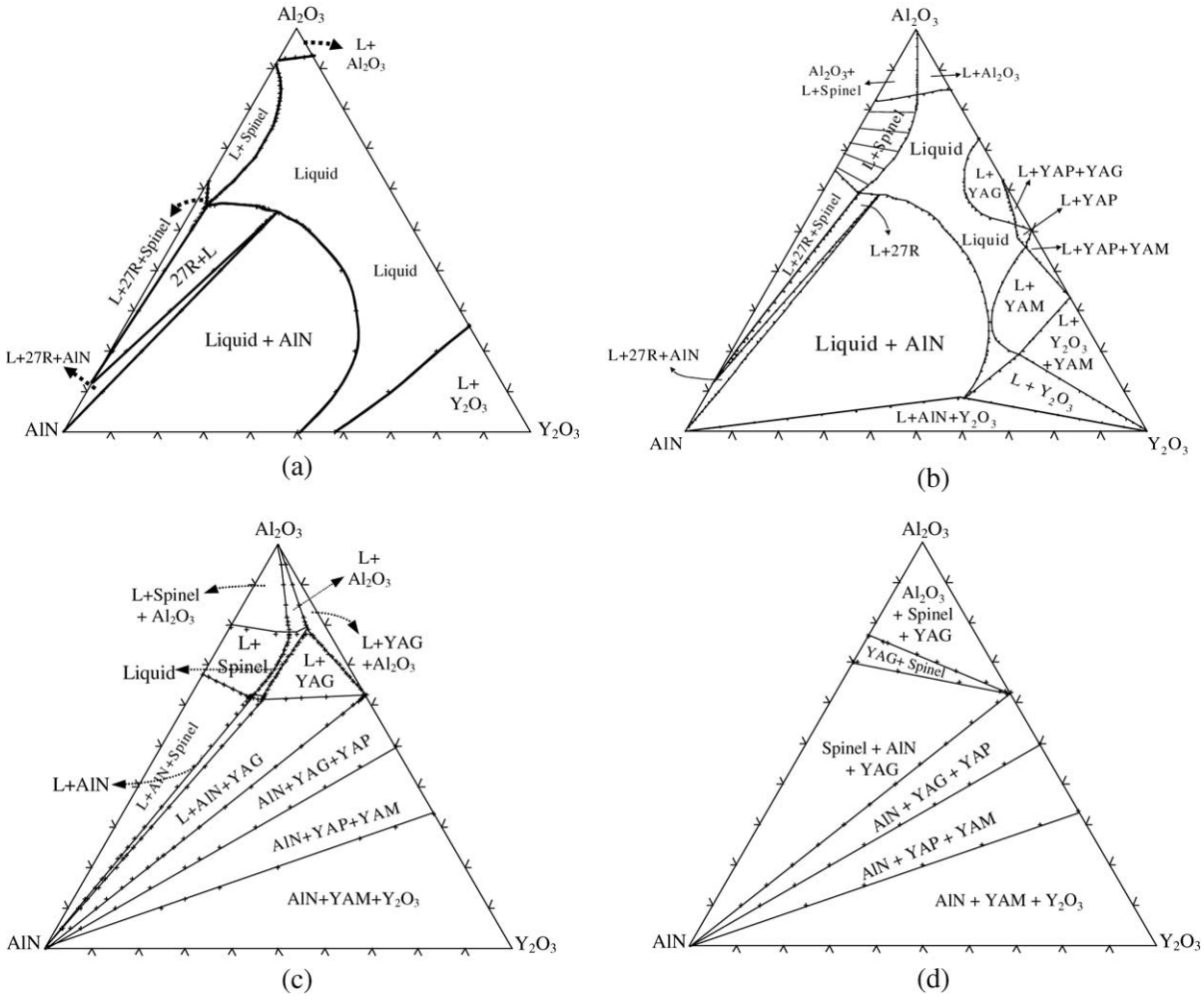

Fig. 1. Isothermal sections of AlN–Al_2O_3–Y_2O_3 system. (a) 2000 °C, (b) 1900 °C, (c) 1800 °C, (d) 1700 °C.

through a 212 μm mesh sieve and were then uniaxially and isostatically pressed to form discs 32 mm in diameter, and a thickness of 3 mm.

All sintering experiments were performed in a horizontal, graphite element resistance furnace equipped for inert atmosphere and the temperature was controlled using a type C thermocouple. The green compacts were placed on a BN setter and then sintered in N_2 at 1700–1950 °C for various hold times followed by furnace cooling.

Densities of the sintered AlN compacts were measured by the Archimedes' principle according to a modified version of the ASTM standard C373-72. The water displacement procedure was accelerated by placing the AlN samples in a closed glass flask containing distilled water, and then evacuating to remove all the air, i.e. complete air removal was assured upon the arresting of air bubbles emerging from samples. The theoretical densities were determined by pycnometry; four representative sintered AlN ceramics from each composition were crushed into powder, and then the volume of each powder was measured in a 10 ml pycnometer bottle with isopropanol. The theoretical density was then calculated using the weight and volume of the powders.

The powders were phase analysed using filtered Cu Kα X-ray radiation. The AlN and the secondary phases were iden-

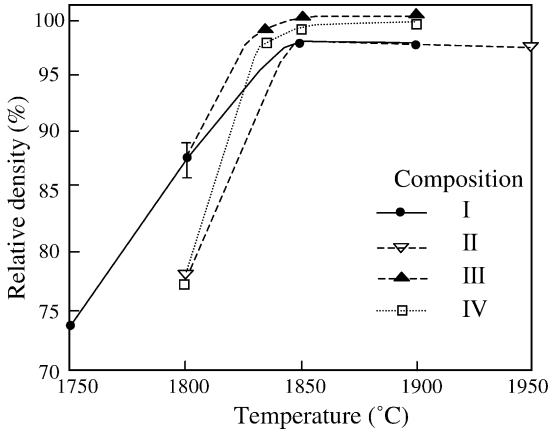

Fig. 2. Relative density of the four compositions as a function of sintering temperature.

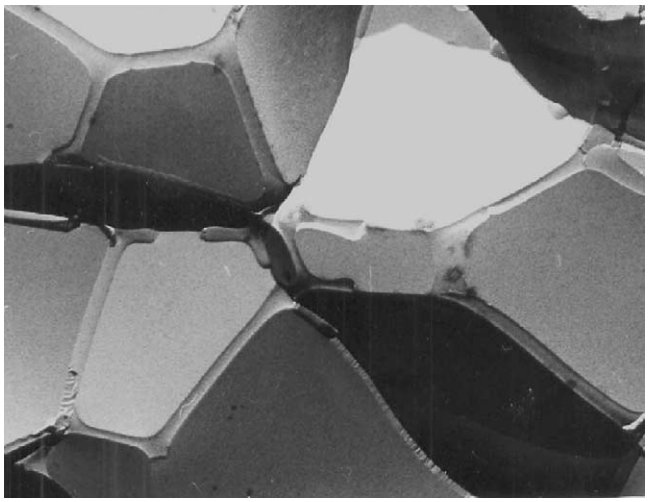

Fig. 3. TEM replica of AlN fracture surface sintered without additive at 1900 °C for 1 h.

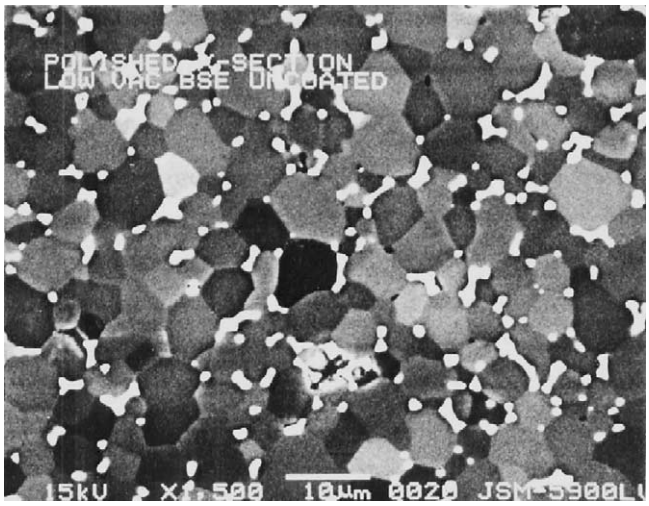

Fig. 4. BS-SEM micrograph of AlN substrates sintered with addition of Y_2O_3.

tified using JCPDS-XRD patterns available in the database of the computer attached to the diffractometer. Both fractured and polished surfaces of sintered AlN were observed by a scanning electron microscope. The typical accelerating voltage used was 10–15 kV. The surface microtopography of samples was also observed by a high resolution TEM using Pt/C replicas. The replicas consisted of a thin Pt/C metal film (1–2 nm thick, consisting of 95% Pt and 5% C) and a 15–20 nm thick supporting C film. Replicas were produced from the fractured surfaces of the samples.

The thermal conductivity measurements of AlN specimens were performed by the Laser-flash technique using a thermal diffusivity measurement facility (Microflash NDT) using a spatially uniform single pulse from a CO_2 laser. The thermal conductivity is then obtained from the thermal diffusivity using the specific heat capacity (C_p), 0.74 J/kg K, according to:

$$k = C_p \rho \delta \tag{2}$$

where k is the thermal conductivity (W/m K), C_p the specific heat capacity (J/kg K), ρ the measured density of AlN (kg/m^3), δ the thermal diffusivity (m^2/s).

4. Results and discussion

Fig. 2 shows the effect of both temperature and time on the sintering of AlN for the compositions under consideration. Basically all compositions reach complete densification after sintering at >1850 °C for 1 h. The experimental observations will be explained by the phase assemblage diagrams (Figs. 6–9). These figures show that all compositions would have formed liquid at this temperature. This liquid promoted

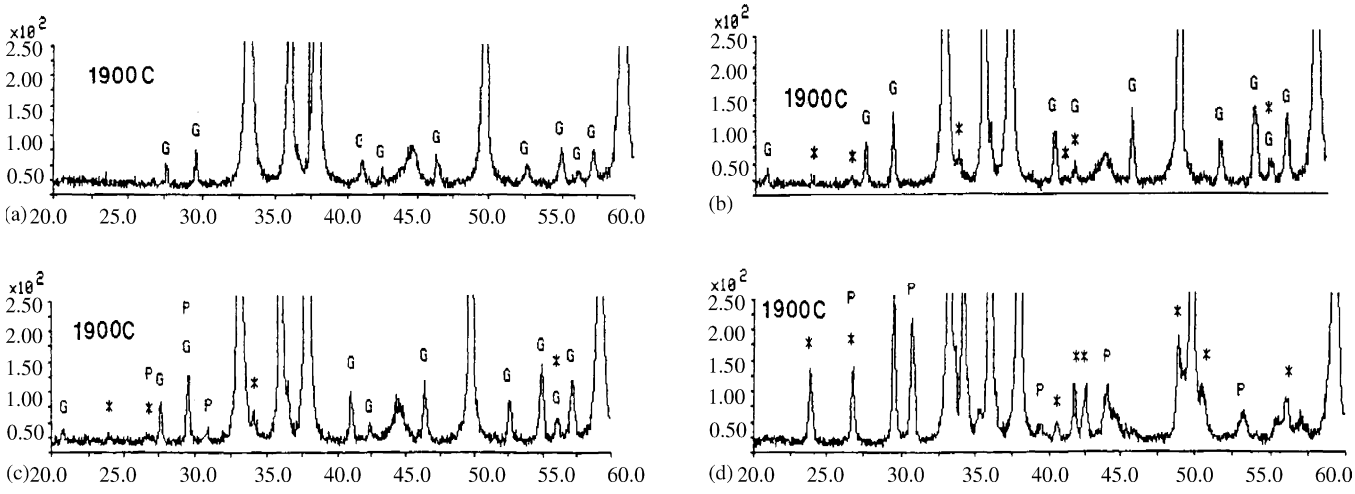

Fig. 5. X-ray powder diffraction patterns of AlN for four compositions, (G): YAG, (P): YAP and (*): YAM.

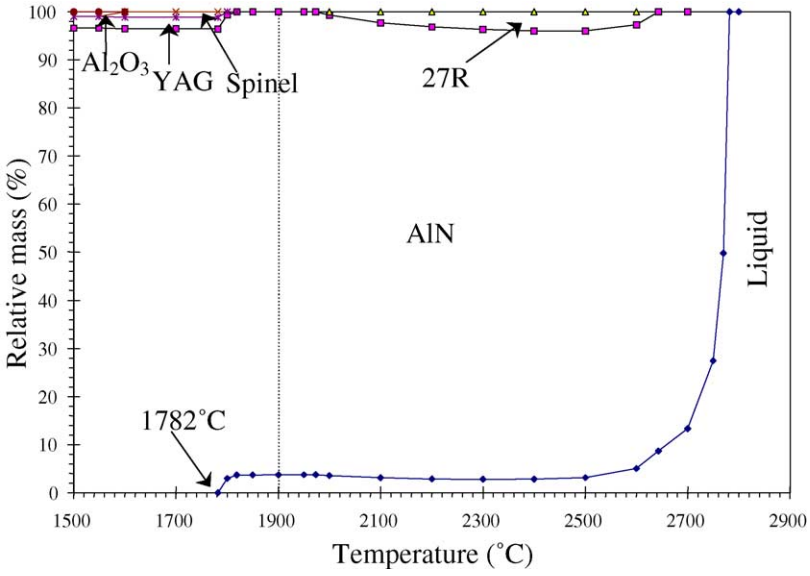

Fig. 6. Phase assemblage of composition I.

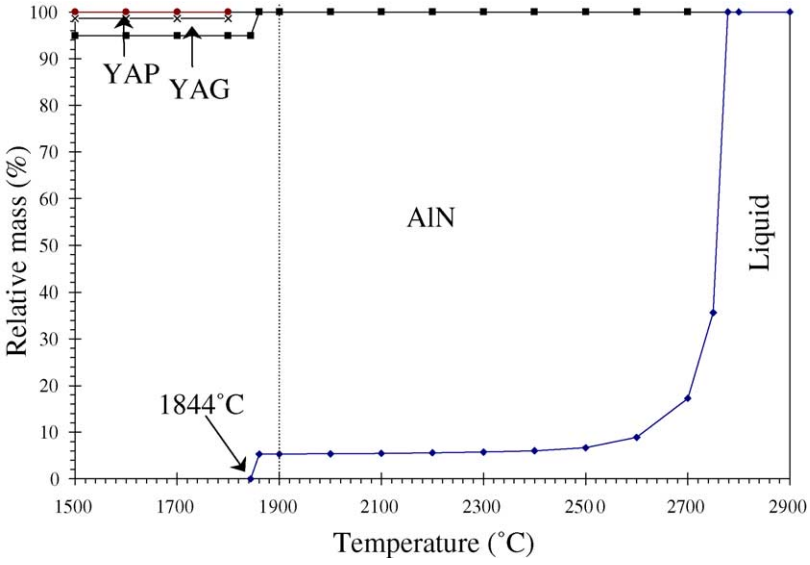

Fig. 7. Phase assemblage of composition II.

the densification noticed in the sintered samples. Also, Fig. 2 shows that composition I reached higher density than the other compositions at 1800 °C, this can be explained by referring to Fig. 6. This figure indicates that this composition starts forming liquid at 1782 °C, which resulted in higher density than the other compositions, which required higher temperatures to form liquid. In all cases sintering reaches completion within 1 h for sintering at 1900 °C because liquid readily exists in all the compositions at this temperature as can be seen in Figs. 6–9.

Sintering for one hour at 1900 °C without Y_2O_3 achieves a density of 99%. A TEM micrograph of this sample is shown in Fig. 3. This high density is due to the formation of an aluminum oxynitride (Al–O–N) liquid by reaction between surface alumina and AlN. The addition of Y_2O_3 promotes more extensive liquid formation due to reaction to form a quaternary liquid (Y–Al–O–N) at lower temperature.

The SEM microstructure of a typical composition containing Y_2O_3 is shown in Fig. 4. The grain boundary distribution of the secondary phase is quite different from that of Fig. 3. The secondary phase (white) shows up at the grain junctions only and not along grain edges.

The addition of Y_2O_3 appears to have a further effect of changing the wetting behaviour of the liquid phase with respect to the AlN grains. Indeed the dihedral angle of the secondary phase at the grain junction is high (>70°). This has a significant effect on the thermal conductivity (k). Jackson et al. [13] suggest that thermal conductivity rises to a maximum and then decreases due to the increase in volume fraction of aluminates with further Y_2O_3 addition.

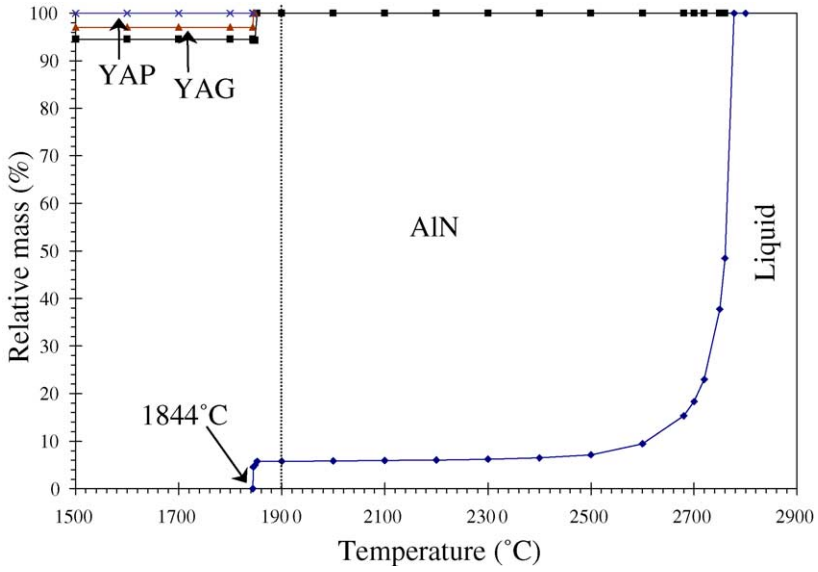

Fig. 8. Phase assemblage of composition III.

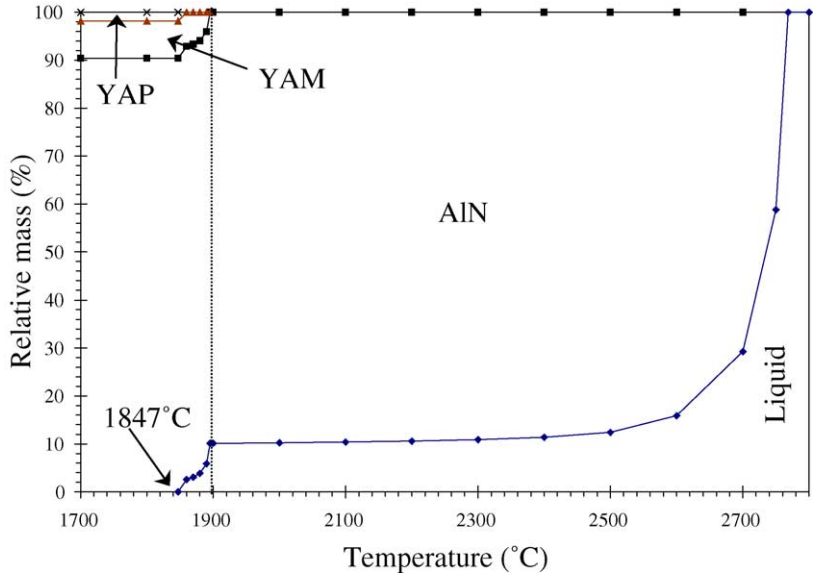

Fig. 9. Phase assemblage of composition IV.

Fig. 5 gives the X-ray powder diffraction patterns for the four compositions after sintering at 1900 °C for one hour. Each composition shows strong peaks associated with AlN in addition to minor peaks associated with the secondary grain boundary phase. These results agree very well with the thermodynamic calculations presented in Figs. 6–9.

Fig. 6 shows, that at room temperature, composition I consists of 96.64 wt.% AlN in addition to 2.38 wt.% YAG and 0.976 wt.% Al_2O_3. The X-ray diffraction at room temperature in Fig. 5(a) showed peaks for AlN and YAG phases only. Al_2O_3 peaks were not detected because the amount of residual Al_2O_3 is very small and below the detection limit of the equipment. Moreover, Al_2O_3 occurs as a thin surface layer on AlN grains. Because of this surface layer and residual spinel, thermal conductivity is very low for this sample, as can be seen in Fig. 10. This means that the amount of added Y_2O_3 was insufficient to fully react with residual Al_2O_3 and to purify the AlN and to complete the oxygen removal from both the lattice and the surface.

Fig. 7 shows that at room temperature composition II consists of 94.96 wt.% AlN, 3.65 wt.% YAG and 1.39 wt.% YAP. In this sample there is more YAG than YAP at room temperature. This agrees with the X-ray pattern shown in Fig. 5(b) where YAG peaks are stronger than those of YAP phase.

Fig. 8 indicates that composition III has a similar phase assemblage to composition II with a difference in the relative amount of each phase. At room temperature composition III consists of 94.53 wt.% AlN, 2.52 wt.% YAG and 2.95 wt.%

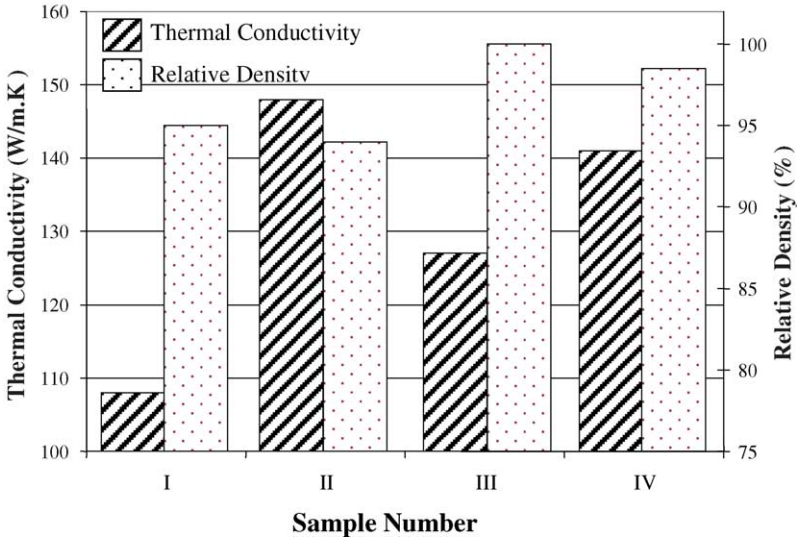

Fig. 10. Variation in thermal conductivity with composition.

YAP. This corresponds well with the X-ray pattern for this sample shown in Fig. 5(c).

Fig. 9 shows the phase assemblage for composition IV and at room temperature this sample is composed of 90.41 wt.% AlN, 7.75 wt.% YAM and 1.84 wt.% YAP. This sample has more YAM than YAP, which agrees with Fig. 5(d), where the diffraction peaks for YAM were stronger than for YAP.

Fig. 10 shows the trend in thermal conductivity of the four compositions along with their relative densities. As discussed above, the amount of secondary phase increases with Y_2O_3 content, hence it is not surprising to find an optimum additive level. The thermal conductivity of the aluminate phase is low (<10 W/m K), hence as the volume fraction increases, a decrease in the overall thermal conductivity is expected. The thermal conductivity of AlN sintered without Y_2O_3 has a significantly lower value of 65 W/m K than material sintered with Y_2O_3. Therefore, the effect of the additive has a major impact on the conductivity in two ways: (a) it removes oxygen from particle surface and (b) a microstructural change occurs as the aluminate de-wets the grain boundaries and segregates to the grain junctions leading to AlN–AlN grain boundary contact. This figure shows, also, that compositions II, III and IV have higher thermal conductivity than composition I because the oxide layer, in these three samples, was consumed to produce YAG, YAP and YAM as secondary phases.

Furthermore, it was shown by the experimental work of Medraj et al. [6] that YAP wets the surface of AlN more than YAG or YAM if all the experimental conditions are considered. Hence, the presence of YAP phase will prevent AlN–AlN surface contact. For this reason the thermal conductivity of compositions II, III and IV varies according to the amount of YAP phase. As discussed above, compositions II, III and IV have 1.39, 2.95 and 1.84 wt.% YAP, respectively, and the corresponding values of thermal conductivity are 148, 127 and 141 W/m K, respectively. Hence, higher YAP content is associated with lower thermal conductivity.

5. Conclusions

An optimised self-consistent thermodynamic database has been developed for AlN–Al_2O_3–Y_2O_3 with the computer system F*A*C*T. This database can now be used to predict the phase relations and various thermodynamic properties in this three-component system, which represents sintering process of AlN.

Thermodynamic modeling of the AlN–Al_2O_3–Y_2O_3 system provides an important basis for understanding the sintering behaviour of aluminum nitride, and explains the experimental results:

- Samples with higher density have lower liquid formation temperature.
- Thermal conductivity is related to the chemistry of the secondary phases.
- Samples with residual Al_2O_3 and/or spinel have lower thermal conductivity.
- Thermal conductivity decreases with the increasing amount of the YAP phase, because YAP wets the AlN surface and prevents AlN–AlN grain boundary formation.

AlN can be sintered to full density both with and without additive using compositional control. However, the Y_2O_3 additive reduces the sintering temperature and performs an important role in the microstructural development. In the absence of Y_2O_3, an Al–O–N phase forms that completely surrounds the AlN grains and is retained as a continuous phase upon cooling to room temperature. This leads to low bulk

thermal conductivity values due to the poor conductivity of this grain boundary phase.

Acknowledgments

This research was carried out with the support of an NSERC Strategic Project grant. The authors thank Dr. H. Vali for the help with TEM work.

References

[1] F. Miyashiro, N. Iwase, A. Tsuge, F. Ueno, M. Nakahashi, T. Takahashi, High thermal conductivity aluminum nitride ceramic substrate and packages, IEEE Trans. Comp. Hybrid. Manuf. Technol. 13 (2) (1990) 313–319.
[2] R. Koba, J. Harris, R. Youngman, M. Mallinger, L.B. Max, Aluminum-nitride packages provide consistent performance, Microwave RF (1997) 156–166.
[3] N. Kuramoto, H. Taniguchi, I. Aso, Development of translucent aluminum nitride ceramics, Ceram. Bull. 68 (4) (1989) 883–887.
[4] J.C. Nipko, C.K. Loong, Phonon excitations and related thermal properties of aluminum nitride, Phys. Rev. B 57 (17) (1998) 10550–10554.
[5] Y. Baik, R.A.L. Drew, Aluminum nitride: processing and applications, Key Eng. Mater. 122–124 (1996) 553–570.
[6] M. Medraj, M. Entezarian, R.A.L. Drew, Wettability of Al_2O_3–Y_2O_3 compounds on aluminum nitride and their role in sintering, Sintering 99 Conference Proceedings, 2000, pp. 307–312.
[7] N.H. Kim, K. Komeya, T. Meguro, Effect of Al_2O_3 addition on phase reaction of AlN–Y_2O_3 system, J. Mater. Sci. 31 (6) (1996) 1603–1608.
[8] M. Hotch, Calculation of ternary, quaternary, and higher-order phase diagrams from binary diagrams and binary thermodynamic data, J. Phase Equilib. 14 (6) (1993) 710–717.
[9] A.D. Pelton, C.W. Bale, W.T. Thompson, F*A*C*T (Facility for the Analysis of Chemical Thermodynamics), McGill University/Ecole Polytechnique, Montreal, 1996.
[10] M. Medraj, R.A.L. Drew, W.T. Thompson, Thermodynamic modeling of the AlN–Al_2O_3–Y_2O_3 system, Can. Metall. Q. 42 (4) (2003) 495–506.
[11] M. Medraj, R. Hammond, W.T. Thompson, R.A.L. Drew, High temperature neutron diffraction of AlN–Al_2O_3–Y_2O_3 system, J. Am. Ceram. Soc. 86 (4) (2003) 717–726.
[12] B. Burton, T.B. Chart, H.L. Lukas, A.D. Pelton, H. Seifert, P. Spencer, Thermodynamic models and data for pure elements and other endmembers of solutions, CALPHAD 4 (19) (1995) 537–553.
[13] T.B. Jackson, A.V. Virkar, K.L. More, R.B. Dinwidie, R.A. Cutler, High-thermal conductivity aluminum nitride ceramics: the effect of thermodynamic, kinetic, and microstructure factors, J. Am. Ceram. Soc. 80 (6) (1997) 1421–1435.